


# Anatomy of the Insertion of the Posterior Inferior Tibiofibular Ligament and the Posterior Malleolar Fracture

Foot & Ankle International®  
2019, Vol. 40(11) 1319–1324  
© The Author(s) 2019  
Article reuse guidelines:  
sagepub.com/journals-permissions  
DOI: 10.1177/1071100719865896  
journals.sagepub.com/home/fai

Malwattage Lara Tania Jayatilaka, MuDr, MRCS<sup>1</sup>,  
Matthew D. G. Philpott MBChB, MRCS<sup>1</sup>,  
Andrew Fisher, BSc (Hons), MSc, PhD<sup>2</sup>,  
Lauren Fisher, BSc (Hons), PhD<sup>2</sup>,  
Andrew Molloy, MBChB, MRCS (Ed), FRCS (Tr&Orth)<sup>1,2</sup>,  
and Lyndon Mason, MBBCh, MRCS (Eng), FRCS (Tr&Orth)<sup>1,2</sup> 

## Abstract

**Background:** Our aim in this study was to identify the extent of the posterior inferior tibiofibular ligament (PITFL) insertion on the posterior tibia and its relation to intra-articular posterior malleolar fractures.

**Methods:** Careful dissection was undertaken on 10 cadaveric lower limbs to identify the ligamentous structures on the posterior aspect of the ankle. The ligamentous anatomy was further compared with our ankle fracture database, specifically posterior malleolar fracture patterns, demonstrating a rotational pilon etiology (Mason and Molloy type 2A and B). Computed tomography imaging was used to measure the dimensions of the fracture fragments.

**Results:** The superficial PITFL was found to have a transverse component and an oblique component. The average size of the tibial insertion was 54.9 mm (95% CI, 51.8, 58.0) from joint line and 47.1 mm (95% CI, 43.0, 51.2) transverse.

From our database of ankle fractures involving the posterior malleolus, 80 Mason and Molloy type 2 fractures were identified for analysis. Of these, 33 were type 2A and 47 were type 2B. The posterolateral fragments had an average size of 26.3 mm (95% CI, 25.0, 27.7) height and 22.1 mm (95% CI, 21.1, 23.1) width. The posteromedial fragments had an average size of 22.0 (95% CI, 18.9, 25.1) height and 19.8 (95% CI, 17.5, 22.0) width.

**Conclusion:** The superficial PITFL insertion on the tibia is broad. In comparison with the average size of the posterior malleolar fragments, the PITFL insertion is significantly larger. Therefore, for a posterior malleolar fracture to cause posterior syndesmotic instability, a ligamentous injury must also occur.

**Clinical Relevance:** Posterior syndesmotic instability results from injury to the PITFL. It has been widely reported that a posterior malleolar fracture will also give rise to posterior syndesmotic instability due to the insertion of the deep PITFL on the posterior tibia. On the contrary, in this paper, we have shown that the superficial PITFL insertion on the tibia is very large, much greater than the average size of the posterior malleolar fragments. Therefore, for a posterior malleolar fracture to cause posterior syndesmotic instability, a ligamentous injury will also have to occur.

**Keywords:** posterior malleolar fracture, intermalleolar ligament, posterior inferior tibiofibular ligament, PITFL, syndesmosis

The increasing understanding of the pathoanatomy and biomechanics of ankle fractures has meant that the management of ankle fractures has evolved considerably in the last decade. As part of this, the treatment of posterior malleolar fractures has been the subject of an increase in research and is a topic of debate in the orthopedic community. Ankle fractures are a common injury representing approximately 10% of all fractures ranging from isolated malleolar fractures to the more complex trimalleolar fractures.<sup>4</sup> Syndesmosis injuries have been shown to occur in up to 20% of ankle fractures. Posterior malleolar fractures occur in up to 40% of ankle fractures.<sup>9</sup>

Traditionally, it was thought that the size of the posterior malleolar fragment was a key prognostic indicator and should dictate management; however, a systematic review by Odak et al stated that most studies showed no association

<sup>1</sup>Aintree University Hospital, Liverpool, United Kingdom

<sup>2</sup>Human Anatomy and Resource Centre, University of Liverpool, Liverpool, United Kingdom

## Corresponding Author:

Lyndon Mason, MBBCh, MRCS (Eng), FRCS (Tr&Orth), Aintree University Hospital, Long Lane, Liverpool, L9 7AL, UK.  
Email: Lyndon.mason@aintree.nhs.uk

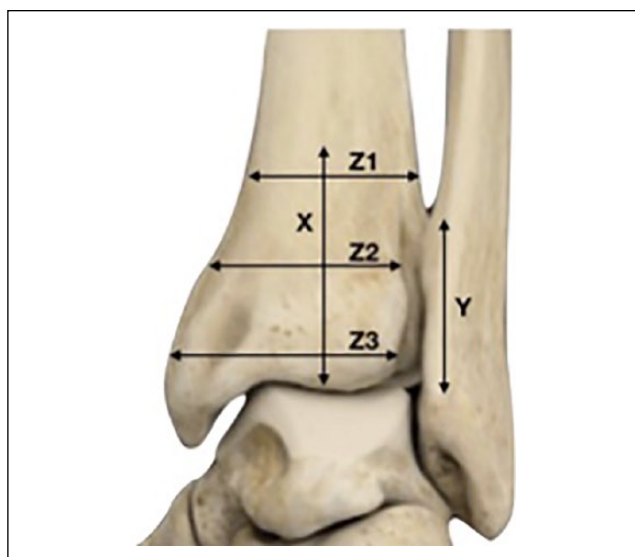


**Figure 1.** Illustration of measurements taken of the posterior inferior tibiofibular ligament in the cadaveric specimens.

between the size of the fragment and long-term outcome.<sup>11</sup> Other studies have shown that fixing the posterior malleolus infers greater syndesmotic stability.<sup>5,10</sup> The posterior inferior tibiofibular ligament (PITFL) has been shown in a cadaveric biomechanical study by Ogilvie-Harris et al<sup>12</sup> to confer up 42% of the strength of the syndesmosis.

The Mason and Molloy classification of posterior malleolus fractures based on computed tomography (CT) scan findings showed that in type 2 fracture patterns (Haraguchi types 1 and 2), only 49% had confirmed syndesmotic instability on testing.<sup>8,9</sup> The Mason and Molloy type 1 injury (Haraguchi type 3) was found to have a 100% syndesmotic disruption, leading to the conclusion that type 1 was an avulsion type injury and type 2 was a rotation pilon injury. The mechanism of injury theorized for the Mason and Molloy type 2 fracture describes an ankle in neutral or plantar flexion with a loaded talus that undergoes a rotational force. We proposed that in order for the Mason and Molloy type 2 injuries to demonstrate syndesmotic disruption, the PITFL footprint should be confined to the fracture fragment. The aim of this cadaveric and radiological analysis study was to examine the anatomy of the insertion of the PITFL and its relation to rotational pilon (Mason and Molloy type 2) injuries.<sup>9</sup>

## Methods

The study was performed in the Human Anatomy Resource Centre at the University of Liverpool and Aintree University Hospital. Tissue was obtained from cadavers bequeathed under the regulations of the Human Tissue Authority, United Kingdom, to the University of Liverpool. We

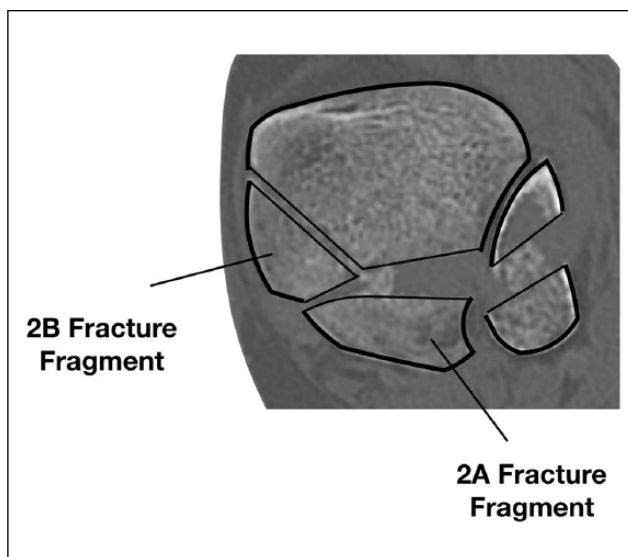


**Figure 2.** A schematic overlaying an axial scan of a type 2 fracture with 2A and 2B fragments present.

initially selected 10 formalin-embalmed cadaveric foot and ankle specimens that had been amputated at the proximal tibia. Each specimen was morphologically normal and showed no signs of previous surgical intervention to the distal tibia or ankle.

The second part of the study consisted of analyzing 3D reformatted CT scans from our prospectively collected ankle fracture database, using digital imaging software (Vue PACS, Carestream, version 11.4.1.0324). All fractures were classified using the Mason and Molloy classification system for posterior malleolar fractures.<sup>9</sup> We separated out from this group patients with Mason and Molloy type 2 fracture patterns (Figure 2).

## Dissection

All 10 specimens were dissected in the same sequence. Initially, the skin along with the subcutaneous fat was removed as 1 layer. The Achilles was dissected from its insertion on the calcaneal tuberosity and the gastrosoleus complex was carefully dissected proximally, and the entire layer was removed. All remaining fat was excised. The deep investing fasciae overlying the deep compartments of the posterior lower limb were excised, followed by the careful removal of the flexor hallucis longus muscle and neurovascular bundles.

Both the peroneal muscles and the tibialis posterior were removed in all specimens by starting distally with the tendons behind the fibula laterally, removing the peroneals from the fibular groove and medially removing the tibialis posterior tendon from the medial malleolar groove. The tendon sheath was incised in the midline on both and the



**Figure 3.** 3D surface rendering of a Mason and Molloy type 2B posterior malleolar fracture, illustrating the measurements taken (see also Table 2).

tendon dissected out, leaving the base of the sheath. We noted that in all the specimens dissected, the PITFL at its most medial extent blended with the tibialis posterior tendon sheath and at its most lateral extent blended with the peroneal tendon sheath.

A digital caliper (calibrated to 0.1 mm) was used to make direct measurements of the PITFL. All specimens were assessed by all 3 dissectors. Digital images were taken in accordance with the Human Tissue Authority license held by the Human Anatomy and Resource Centre. All 10 specimens were measured in an identical sequence as demonstrated in Figure 1.

### Radiographic Analysis

All patients entered into our ankle fracture database were evaluated. As per protocol in our department, all posterior malleolar fractures underwent CT imaging. All patients identified to have sustained a type 2 Mason and Molloy fracture underwent further analysis. The measurements of the posterior malleolar fracture fragments were completed using our departmental imaging software (Vue PACS, Carestream, version 11.4.1.0324). The measurements taken are shown in Figure 3. Syndesmotic diastasis was defined as a >5-mm gap between the fibula and incisura on CT, and further tested intraoperatively on live screening.<sup>16</sup>

### Results

The PITFL was present in all anatomical specimens. The PITFL insertion on the tibia was found to be broad. In all specimens the PITFL blended with the tibialis posterior tendon sheath medially (Figure 4). Laterally the PITFL blended into the peroneal tendon sheath. Proximally the PITFL split into 2 separate insertions as it inserted on to the tibia, an

oblique insertion and a transverse insertion. This was found in all 10 specimens and has been labeled in our results as the oblique insertion and the transverse insertion. The average length of the oblique insertion was 54.9 mm (95% CI, 51.8, 58.0) from the joint line and the average length of the transverse insertion was 41.0 mm (95% CI, 36.5, 45.5) from the joint line. Quantification of the extent of PITFL insertion is illustrated in Table 1. The intermalleolar ligament was present in all specimens, with the ligament extending from the fibula to insert on the lateral component of the tibialis posterior sheath at its most distal extent.

From our department's prospectively collected database of ankle fractures involving the posterior malleolus, 80 Mason and Molloy type 2 fractures were identified for analysis. Of these, 33 were type 2A and 47 were type 2B. The fragment sizes are illustrated in Table 2. In comparing the demographics of the fracture types, there were no significant differences found. In regard to syndesmosis instability, the overall rate of injury with type 2 fractures was 51.3%. These results are illustrated in Table 3.

### Discussion

The anatomy of the ligaments of the tibiofibular syndesmosis has been the subject of a number of cadaveric and radiological studies. Golano et al<sup>6</sup> described the PITFL from arthroscopic cadaveric studies as having superficial fibers and deep transverse fibers. They described the deep transverse ligament as a true labrum that deepens the tibial articular surface and increases the tibial concavity. The deep transverse ligament as a part of the PITFL or a distinct ligament of its own is debated across the literature. Bartonicek<sup>1</sup> described that there was no reason it should be considered a separate ligament. Ebraheim et al<sup>3</sup> acknowledged the close proximity of the insertion points onto the fibula of the ligament fibers, but detailed that there was a fibrofatty connective tissue mass between the ligaments and described it as a separate inferior transverse ligament.

The superficial fibers have been described by Ebraheim et al<sup>3</sup> as being oriented between 20 degrees to the horizontal plane and 85 degrees to the sagittal plane. They found that the PITFL was the thickest of the tibiofibular syndesmotic ligaments. They also described the shape of the ligament as triangular, narrowing onto the insertion onto the fibula, whereas Williams et al<sup>15</sup> described it as being more trapezoidal in shape. Our findings agree with those of Williams et al, with a trapezoidal insertion point on the fibula, although we would go further in that the insertion was confluent with the peroneal tendon sheath.

Williams et al<sup>15</sup> described the PITFL insertion on the tibia as having superficial fibers attaching broadly along the distolateral margin, with a surface area of 84.5 mm<sup>2</sup> on average. They also described deep fibers attaching specifically on the posterolateral tibial tubercle with an average

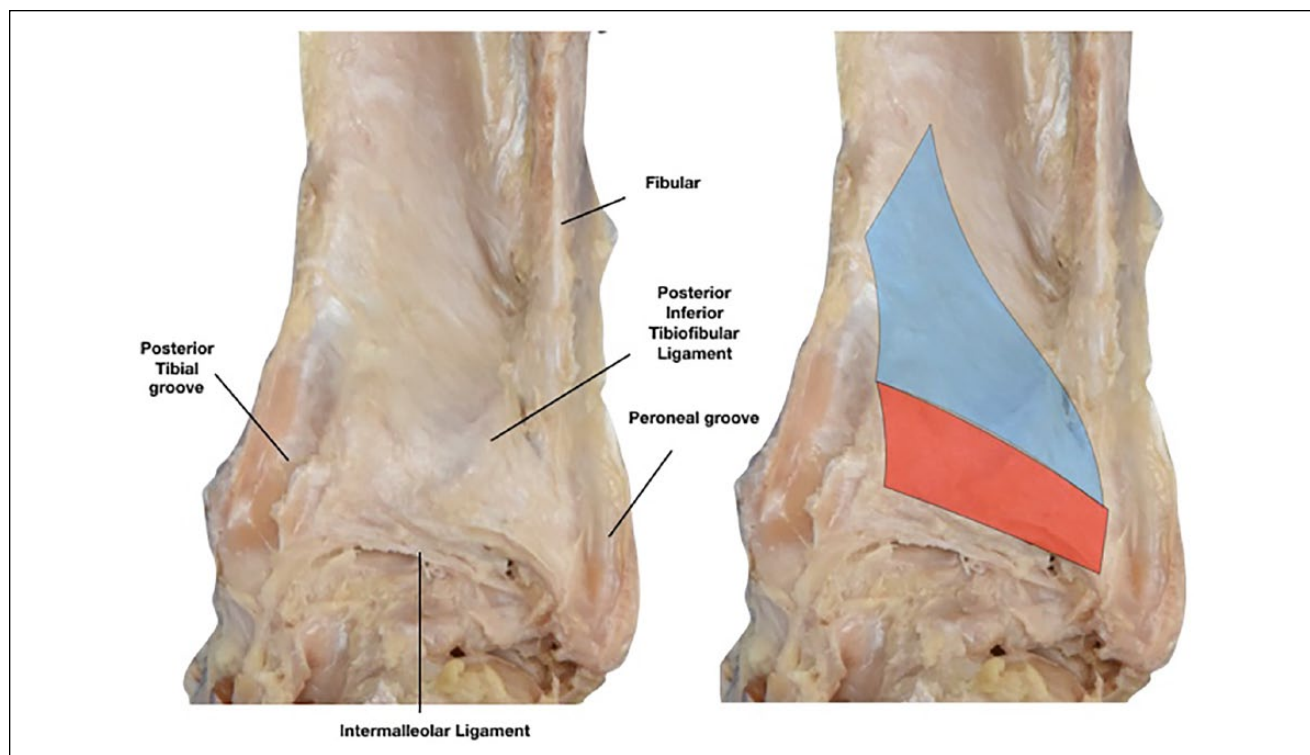


**Figure 4.** Cadaveric dissection of the posterior aspect of the tibia illustrating the broad insertion of the posterior inferior tibiofibular ligament (PITFL) and its medial extent. The PITFL had 2 separate insertions on the tibia (shading).

**Table 1.** Measurements Taken of the PITFL Origin and Insertion as Illustrated in Figure 1.

Measurement <sup>a</sup>	Mean (mm)	95% CI	
		Lower	Upper
Oblique insertion	54.9	51.8	58.0
Transverse insertion	41.0	36.5	45.5
Z1	24.6	22.2	26.9
Z2	33.8	30.7	36.8
Z3	47.1	43.0	51.2
Y	39.6	36.2	43.1
Intermalleolar ligament	30.3	28.1	32.6

Abbreviation: PITFL, posterior inferior tibiofibular ligament.

<sup>a</sup>Oblique insertion and transverse insertion correspond to the 2 separate insertions of PITFL found on cadaveric dissection.

surface area of 52.2 mm<sup>2</sup>. We were unable to differentiate deep and superficial fibers inserting into the tibia on our dissection; however, the distal-lateral extent of the tibia had a thicker ligamentous layer that thinned as it spread across the tibia. In our study, we have identified a much larger superficial deltoid insertion, which is split into separate oblique (inserting proximally) and transverse (inserting medially) sections, inserting as far proximal as 58 mm from the joint line. This is similar to the description by

**Table 2.** Dimensions of the Posterior Malleolar Fracture as Measured From the 3D Surface Rendering of 2-mm-Slice Preoperative Computed Tomography Scans Obtained in Our Department.

Fragment	No.	Mean Dimensions, mm (95% CI)	
		X	Y
Posterolateral fragment	80	26.3 (25.0, 27.7)	22.1 (21.1, 23.1)
Posteromedial fragment	47	22.0 (18.9, 25.1)	19.8 (17.5, 22.0)

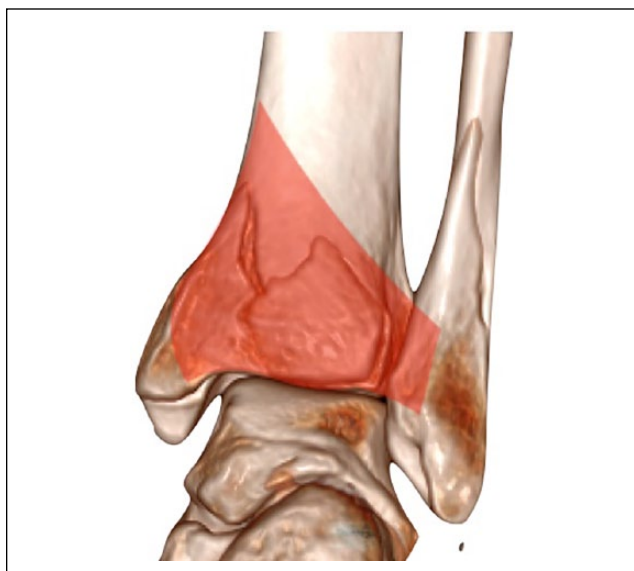
Bartonicek,<sup>1</sup> who described an upper part of the ligament, a more horizontally oriented lower part, and described the overall shape of the PITFL as similar to that of the anterior inferior tibiofibular ligament (AITFL).

Previous studies have described the important role the PITFL has on the stability of the syndesmosis.<sup>2,12</sup> Clanton et al,<sup>2</sup> in a biomechanical analysis of individual syndesmotomic ligaments, detailed that the PITFL is an important structure in controlling internal rotation. This would explain why, when the PITFL is injured in Mason and Molloy type 1 injuries, internal rotation stress testing using live or arthroscopic screening identifies a quarter of isolated posterior syndesmotomic disruptions.<sup>9</sup> Gosselin-Papadopoulos et al<sup>7</sup>



**Table 3.** Mason and Molloy Injury Type, Comparing Demographics, Syndesmotic Instability, and Lauge-Hansen Injury Mechanism.

Type	No.	Average Age, y (Range)	Syndesmosis Instability (%)	Pronation/Supination Injury
2A	33	50.2 (21-87)	23 (69.7)	13/20
2B	47	46.6 (17-90)	18 (38.3)	20/27
Overall	80	48.1 (17-90)	41 (51.3)	33/49

**Figure 5.** Schematic illustration of a type 2B posterior malleolar fracture with a superimposed posterior inferior tibiofibular ligament showing the relatively larger size of the ligament compared with the fracture fragment size.

also described a test where stressing the fibula posterolaterally under direct visualization showed the greatest degree of displacement when the PITFL was sectioned.

Our study has highlighted the anatomy of the PITFL, in particular its footprint on the tibia, and correlated this with CT imaging of posterior malleolus fractures of the ankle (Figure 5). To our knowledge, this is the first paper to do this. The results of this study help to strengthen the hypothesis that Mason and Molloy type 2 fractures are rotational pilon injuries and not avulsion injuries as described by Haraguchi et al<sup>8</sup> (type 1). Interestingly, the rate of syndesmotic injury was greater for type 2A fracture patterns than type 2B fracture patterns, even though the type 2B fractures had a greater extent of bone injury. Warner et al described 96% of PITFL injuries as posterior malleolar disruptions on MRI.<sup>14</sup> These were not described as fractures, but a high signal between the ligament and bone, in keeping with a peeling off of the ligament. Accepting the pilon etiology of the type 2 fractures, for a syndesmotic injury to occur, the PITFL also has to fail. The size of a fragment is therefore irrelevant. The increase in syndesmotic instability in type 2A compared with type 2B is likely due to the rotating talus

peeling off the ligament as it continues to rotate, compared with the bone failing and superficial PITFL being preserved in type 2B fractures.

Vosoughi et al<sup>13</sup> described a posteromedial avulsion fragment associated with posterior malleolar fractures in pronation injuries, which they believed was due to the pull of the intermalleolar ligament. We have identified the intermalleolar ligament in all specimens, showing that its insertion was predictably inferior to the PITFL, inserting on the lateral component of the tibialis posterior sheath at its most distal extent. The current study supports the theory of the posterior medial fracture avulsion in small fragments at the insertion point of the intermalleolar ligament.

We accept that our study has limitations. Although this is the largest published series of this subgroup of fractures, further numbers are necessary for robust statistical analysis. The number of cadavers were limited to 10, and we acknowledge that a larger number would have given us a better understanding of variability; however, the 95% confidence intervals were small on all measurements.

## Conclusion

The PITFL insertion on the tibia is broad. In comparison to the average size of the posterior malleolar fragments, the PITFL insertion is significantly larger. Thus, for a posterior malleolar fracture to cause posterior syndesmotic instability, a ligamentous injury would also have to occur. We believe that this finding explains the finding by Mason and Molloy that only 49% of type 2 injuries had a syndesmotic injury on testing,<sup>9</sup> which we theorize is due to the fact that these are rotational pilon fractures, and with the PITFL having such a broad insertion, it is not avulsed in all cases.


## Declaration of Conflicting Interests

The author(s) declared the following potential conflicts of interest with respect to the research, authorship, and/or publication of this article: The authors report a grant from the British Orthopaedic Foot & Ankle Society, during the conduct of the study. ICMJE forms for all authors are available online.

## Funding

The author(s) disclosed receipt of the following financial support for the research, authorship, and/or publication of this article: Funding was provided through a grant given by the British Orthopaedic Foot & Ankle Society.

## ORCID iD

Lyndon Mason, MBBCh, MRCS (Eng), FRCS (Tr&Orth),   
<https://orcid.org/0000-0002-0371-3183>

## References

1. Bartonicek J. Anatomy of the tibiofibular syndesmosis and its clinical relevance. *Surg Radiol Anat.* 2003;25(5-6):379-386.
2. Clanton TO, Williams BT, Backus JD, et al. Biomechanical analysis of the individual ligament contributions to syndesmototic stability. *Foot Ankle Int.* 2017;38(1):66-75.
3. Ebraheim NA, Taser F, Shafiq Q, Yeasting RA. Anatomical evaluation and clinical importance of the tibiofibular syndesmosis ligaments. *Surg Radiol Anat.* 2006;28(2):142-149.
4. Elsoe R, Ostgaard SE, Larsen P. Population-based epidemiology of 9767 ankle fractures. *Foot Ankle Surg.* 2018;24(1):34-39.
5. Gardner MJ, Brodsky A, Briggs SM, Nielson JH, Lorich DG. Fixation of posterior malleolar fractures provides greater syndesmototic stability. *Clin Orthop Relat Res.* 2006;447:165-171.
6. Golano P, Mariani PP, Rodriguez-Niedenfuhr M, Mariani PF, Ruano-Gil D. Arthroscopic anatomy of the posterior ankle ligaments. *Arthroscopy.* 2002;18(4):353-358.
7. Gosselin-Papadopoulos N, Hebert-Davies J, Laflamme GY, et al. Intraoperative torque test to assess syndesmosis instability. *Foot Ankle Int.* 2018;40(4):408-413.
8. Haraguchi N, Haruyama H, Toga H, Kato F. Pathoanatomy of posterior malleolar fractures of the ankle. *J Bone Joint Surg Am.* 2006;88(5):1085-1092.
9. Mason LW, Marlow WJ, Widnall J, Molloy AP. Pathoanatomy and associated injuries of posterior malleolus fracture of the ankle. *Foot Ankle Int.* 2017;38(11):1229-1235.
10. Miller AN, Carroll EA, Parker RJ, Helfet DL, Lorich DG. Posterior malleolar stabilization of syndesmototic injuries is equivalent to screw fixation. *Clin Orthop Relat Res.* 2010;468(4):1129-1135.
11. Odak S, Ahluwalia R, Unnikrishnan P, Hennessy M, Platt S. Management of posterior malleolar fractures: a systematic review. *J Foot Ankle Surg.* 2016;55(1):140-145.
12. Ogilvie-Harris DJ, Reed SC, Hedman TP. Disruption of the ankle syndesmosis: biomechanical study of the ligamentous restraints. *Arthroscopy.* 1994;10(5):558-560.
13. Vosoughi A, Jayatilaka M, Fischer B, Molloy A, Mason L. CT Analysis of the posteromedial fragment of the posterior malleolar fracture. *Foot Ankle Int.* 2019;40(6):648-655.
14. Warner SJ, Garner MR, Schottel PC, Hinds RM, Loftus ML, Lorich DG. Analysis of PITFL injuries in rotationally unstable ankle fractures. *Foot Ankle Int.* 2015;36(4):377-382.
15. Williams BT, Ahrberg AB, Goldsmith MT, et al. Ankle syndesmosis: a qualitative and quantitative anatomic analysis. *Am J Sports Med.* 2015;43(1):88-97.
16. Yeung TW, Chan CY, Chan WC, Yeung YN, Yuen MK. Can pre-operative axial CT imaging predict syndesmosis instability in patients sustaining ankle fractures? Seven years' experience in a tertiary trauma center. *Skeletal Radiol.* 2015;44(6):823-829.